ORIGINAL PAPER

Spirometric and flow-volume curve analysis in rats, and optimal parameters for estimating obstructive impairment

Tetsuri Kondo · Toshimori Tanigaki ·
Chizuko Tsuji · Hidehiro Watanabe

Abstract We obtained flow-volume (*F-V*) curves in anesthetized rats by applying positive pressure on the body surface. To obtain the best curve, tracheal intubation with either a 12 or 13 gauge catheter and a surface pressure greater than 56 cmH$_2$O was necessary. Peak expiratory flow rate (PEFR) and forced vital capacity (FVC) were shown to be optimal parameters for estimation of bronchoconstriction induced by methacholine inhalation while FEV$_{0.05}$ (forced expiratory volume at 0.05 s) and FEV$_{0.10}$ were of limited usefulness for this purpose. The descending segment of the *F-V* curve consisted of two or three phases, with later phases shortened during bronchoconstriction. In conclusion, PEFR and FVC are optimal parameters for estimation of bronchoconstriction in rats. The decreases in PEFR and FVC may reflect constriction in large and smaller airways, respectively.

Keywords Flow limitation · Lung function test · Small animals

Introduction

Chronic pulmonary disease is associated with alterations in pulmonary function. In studies in animal models, however,

T. Kondo (✉) · H. Watanabe
Department of Respiratory Medicine, Tokai University Hachioji
Hospital, Hachioji, Tokyo 192-0032, Japan
e-mail: tetsuri@hachioji-hosp.tokai.ac.jp

T. Tanigaki
Department of Clinical Health Science, Tokai University School
of Medicine, Isehara, Kanagawa 259-1193, Japan

C. Tsuji
Department of Physiology, Tokai University School
of Medicine, Isehara, Kanagawa 259-1193, Japan

pulmonary function has been less utilized to assess pulmonary disease than pathologic or cytologic analysis. It is difficult to achieve accuracy noninvasively when measuring pulmonary function in small animals [1]. This is due primarily to the significant difference in airway mechanics between small animals and humans. For example, small human airways—those less than 2 mm in diameter—lack cartilage and are structurally vulnerable, the largest airway in rats, the cartilaginous trachea, is also approximately 2 mm in diameter. Furthermore, airway resistance in rats must be substantially higher than that in humans since the resistance to linear flow in a tube is inversely proportional to the fourth power of its radius.

Spirometry and flow-volume (*F-V*) curves are the ones most frequently used in clinical practice, and they enable separate assessment of the function of large and small airways. A few previous studies [2–5] have suggested that *F-V* curves in rats, mice, and hamsters resemble those of humans. However, a standard method for producing forced expiration in animals has not been established, and there has been no precise analysis of the *F-V* curve of small animals. In this study we outline a method for obtaining *F-V* curves in rats and describe the changes resulting from inhalation of a bronchoconstrictive agent. The results allowed us to define the optimal parameters for estimation of obstructive impairment in small animals.

Methods

This study has been approved by the Institutional Animal Care and Use Committee at Tokai University.

The subjects were 15 male, 8-week-old, Wistar strain rats with body weights between 230 and 380 g (provided

by CLEA Japan, Tokyo). They were anesthetized with 0.05 mg g^{-1} intraperitoneal (ip) pentobarbital.

Figure 1 shows the device used for forced expiration and spirometric measurements. This is a tightly sealed chamber with a volume of 650 ml. Rats were placed in the supine position and a negative pressure (-15 cmH$_2$O, 0.02 s) was intermittently applied to the box to coincide with their spontaneous respiratory rhythm. Between negative pressures, the box was opened to the atmosphere. Rhythm of spontaneous respiration was then replaced by that of mechanical ventilation. In this condition a negative pressure (-15 cmH$_2$O, 0.5 s) followed by a sudden positive pressure (75 cmH$_2$O, 0.75 s, >60 l min^{-1}) was sequentially applied. The positive pressure was generated by blowing air (30 l min^{-1}) against a water-filled tank (Fig. 1). To prevent initial pressure drop, a 40 l reservoir tank was placed between the tank and the air-tight box. The negative pressure was produced by suctioning air through a water-filled tank. All the solenoid valves were controlled by an electronic circuit.

Measurements were made using a pneumotachometer (TV-241T, Nihon Kohden, Tokyo, Japan) with linearity confirmed up to 200 ml s^{-1}. The expiratory volume was obtained by numerical integration of the expired flow. The data were stored in the PowerLab System (ADInstrument, Sydney, Australia) with 2.0 kHz sampling rate and were then analyzed.

For tracheal intubation we used commercially available plastic catheters in 12, 14 (Angiocath, Becton-Dickinson, NJ, USA), and 13 gauge (G) (Abbocath-T, Abbot Ireland, Sligo, Ireland) sizes. They were cut to 4.5 cm lengths. The 13 and 14G catheters were satisfactory for oral intubation. However, 12G catheters were too large for oral intubation
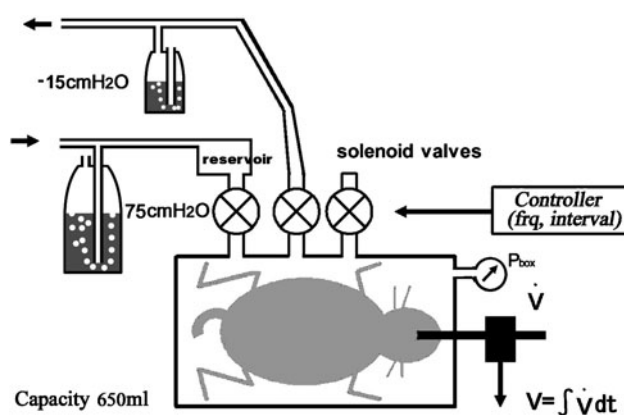
Fig. 1 The system to develop forced expiration was a tightly sealed box with a volume of 650 ml. After intermittent application of -15 cmH$_2$O to the box, a positive pressure of ~ 75 cmH$_2$O was suddenly applied to body surface. The positive pressure was generated by blowing air against a water-filled tank. The negative pressure was generated by suctioning air through a water-filled tank. All the solenoid valves were controlled by an electronic circuit

and were therefore used after tracheostomy. As discussed later, the caliber of the tracheal tube has a significant effect on the F-V curve in rats. For this reason, we measured the exact OD, ID, and resistance of the plastic catheters initially.

Experimental protocols were as follows:

1. *Effect of tracheal tube caliber on the F-V curve.* The rats were orally intubated with a 13 or 14G catheter and five to seven cycles of forced expiration were completed to obtain the F-V curves. Cervical tracheostomy was then performed with insertion of a 12G catheter, and the same procedure repeated.
2. *Effect of afferent and efferent signals from the vagus nerves on the F-V curve.* Forced expiration was induced to obtain F-V curves in the rats before and after bilateral vagus nerve transection in the neck.
3. *Effect of driving pressure on the F-V curve.* Forced expiration was induced to obtain F-V curves in the rats using positive pressures of 70, 64, and 56 cmH$_2$O in the chamber.
4. *Effect of a bronchoconstrictive agent on the F-V curve.* The rats were moved to another sealed box and exposed to methacholine (Mch) mist generated by ultrasonic nebulizer (Soniclizer, Atom, Japan) for 2 min. Immediately after the exposure, five to seven cycles of forced expiration were completed to obtain the F-V curves. After saline control, the Mch concentration was increased from 0.5 to 1.0, 2.0, and 4.0 mg ml^{-1}, progressively doubling the dose.
5. *Effects of respiratory muscle activity on the F-V curve.* In two rats, after experimental protocol 1, ip pancuronium (2.0 mg kg^{-1}) was administered, and forced expiration was measured for five to seven cycles.

Statistical analysis was performed using a repeated-measure ANOVA. If the P value was less than 0.05, the result was considered significant.

Results

By definition, 25 mm (1 in) divided by the gauge number is the diameter of the catheter. The diameters of the catheter should have been 2.1 mm (12G), 1.9 mm (13G), and 1.8 mm (14G). Measured actual diameters of the catheters were as follows: OD 2.7 mm (12G), 2.3 mm (13G), and 2.0 mm (14G), and ID 2.0 mm (12G), 1.8 mm (13G), and 1.4 mm (14G). The measured resistances of the catheters were 0.22 cmH$_2$O ml^{-1} s^{-1} (12G), 0.35 cmH$_2$O ml^{-1} s^{-1} (13G), and 0.53 cmH$_2$O ml^{-1} s^{-1} (14G). Thus, the resistance of the 14G catheter was almost twice that of the 12G.

The position of the tracheal tube has a substantial effect on the shape of the F-V curve, as discussed in detail

elsewhere [4]. Figure 2a shows the F-V curves using each caliber of tracheal catheter. As noted in two consecutive trials, the F-V curve using the same caliber of tracheal catheter showed good reproducibility. However, the shape of the F-V curves differed considerably depending on the catheter size. Each of the F-V curves consisted of four phases. The flow rose steeply initially (first phase), and declined steeply (second phase) after reaching peak flow. Following the second phase, the flow decreased slowly (third phase), and finally it decreased steeply again (fourth phase). The fourth phase was observed in approximately half of the trials. Compared with the F-V curve using the 12G catheter, the peak flow using the 13G catheter occurred later, with this delay much more pronounced in the curves using the 14G catheter.

Figure 2b shows the mean peak expiratory flow rate (PEFRs) using each catheter. They were (mean ± SD) 107.5 ± 15 ml s^{-1} (12G), 103 ± 21 ml s^{-1} (13G), and 107 ± 16 ml s^{-1} (14G). Mean PEFRs using any size catheter were not significantly different. Figure 2c shows the forced vital capacity (FVC) for each catheter size. They were 7.51 ± 1.30 ml (12G), 7.96 ± 1.60 ml 13G), and 7.93 ± 1.00 ml (14G). FVC was also not dependent on catheter size. Figure 2d shows the position of peak flow at expired volume in relation to the catheter size. They were 1.5 ± 0.36 ml (12G), 1.7 ± 9.5 ml (13G), and 3.4 ± 0.6 ml (14G). There was no significant difference between the PEFR position in the F-V curve using 12G and 13G catheters. The PEFR position using a 14G catheter was significantly later in the F-V curve than when using a 12G or 13G catheter.

Figure 3 shows flow-time (F-T) curves using 12G, 13G, and 14G catheters (Fig. 3a), and forced expiratory volumes at 0.05 s (FEV$_{0.05}$) (Fig. 3b) and 0.10 s (FEV$_{0.10}$) (Fig. 3c),

each expressed as a percentage of FVC. The shapes of the F-T curves using 12G and 13G catheters resembled each other. In contrast, PEFR was delayed when using the 14G catheter. It should be noted that, in all of the trials, expiratory flow reached its peak while driving pressure (P_{box}) was still increasing (upper traces in Fig. 3a).

In clinical practice FEV$_{1.0}$/FVC is the parameter widely used to reflect pulmonary obstructive impairment. Since forced expiration terminated within almost 2 s in rats, we evaluated FEV$_{0.05}$/FVC and FEV$_{0.10}$/FVC instead of FEV$_{1.0}$/FVC as alternative parameters. Their values are shown in Fig. 3b, c: mean FEV$_{0.05}$/FVC values were $45.5 \pm 6.8\%$ (12G), $43.4 \pm 4.0\%$ (13G), and $44.5 \pm 5.3\%$ (14G), and mean FEV$_{0.10}$/FVC were $73.2 \pm 6.1\%$ (12G), $72.6 \pm 7.6\%$ (13G), and $78.9 \pm 5.0\%$ (14G). There were no significant differences in FEV$_{0.05}$/FVC using any size catheter; similarly no significant differences were seen in FEV$_{0.10}$/FVC.

The following studies were confined to the use of 12G catheters with tracheostomy. PEFRs before and after bilateral vagus nerve transection were 107.0 ± 14.5 and 107.0 ± 15.4 ml s^{-1}, respectively. They were not significantly different. The FVCs before and after bilateral vagotomy were 7.76 ± 1.00 and 7.74 ± 1.09 ml, respectively, with no significant difference between them.

With the use of a 12G catheter, the shape of the F-V curve was not altered by a change in driving pressure at forced expiration. As seen in Fig. 4, mean PEFRs corresponding to individual driving pressures were 107 ± 15 ml^{-1} s^{-1} (70 cm H$_2$O), 108 ± 17 ml^{-1} s^{-1} (64 cmH$_2$O), and 107 ± 19 ml^{-1} s^{-1} (56 cmH$_2$O). FVCs were 7.74 ± 1.09 ml (70 cm H$_2$O), 7.73 ± 0.90 ml (64 cmH$_2$O), and 7.71 ± 0.94 ml (56 cmH$_2$O). There were no significant differences either

Fig. 2 F-V curves using tracheal catheters of three different sizes. Reproducibility of the F-V curves was good using any size catheter (a). Peak expiratory flow rate was not affected by the size of the tracheal catheter (b). FVC was not affected by the size of the tracheal catheter (c). When a 14G catheter was used, the peak flow was delayed (c). Mean ± SD. $P < 0.05 versus 12G, *P < 0.05 versus 13G. All four phases of the F-V curve—initial steep increase (first), steep decrease (second), slow decrease (third), and steep decrease (fourth)—are depicted in a for the 12G catheter
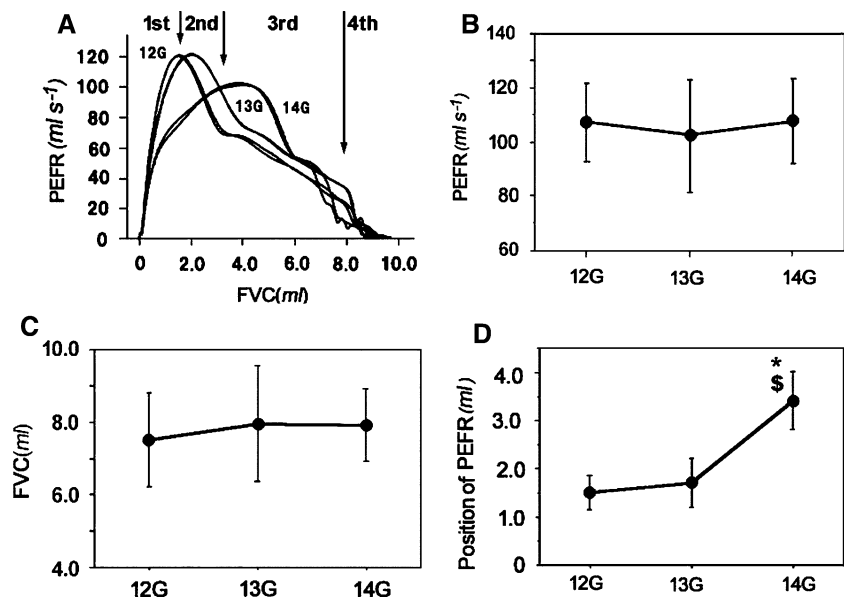
Fig. 3 Expiratory peak flow was reached while the driving pressure (P_{box}) was still rising (**a**). There were no significant differences in $FEV_{0.05}/FVC$ using any size catheter (**b**) or in $FEV_{0.10}/FVC$ (**c**). Values are mean ± SD
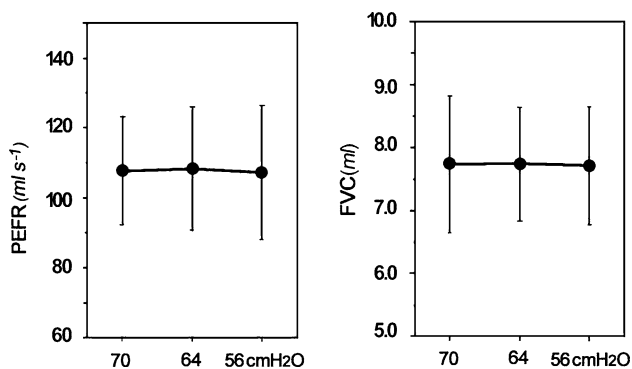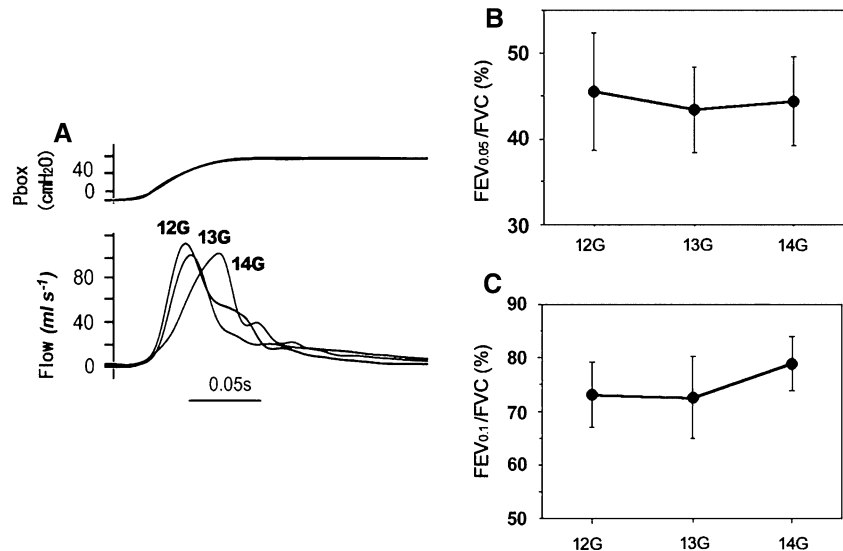
Fig. 4 PEFR and FVC of forced expiration remained unchanged when the driving pressure exceeded 56 cmH$_2$O. Values are mean ± SD

Fig. 5 Changes in the shape of the *F-V* curves for Mch inhalations of different concentrations. Both PEFR and FVC decreased with progressive increases in Mch concentration

among PEFRs or FVCs for each driving pressure. Although not shown in Fig. 4, $FEV_{0.05}$ and $FEV_{0.10}$ driven by 64 or 56 cmH$_2$O were not significantly different from those driven by 70 cmH$_2$O.

Figure 5 shows shapes of the *F-V* curves after inhalation of Mch of different concentrations. Both PEFR and FVC decreased with progressive increases in Mch concentration. There was a tendency for all the phases except for the fourth phase to decrease with progressive increases in Mch concentration.

Figure 6 quantitatively depicts changes in the *F-V* curve during Mch inhalation. Both PEFR (Fig. 6a) and FVC (Fig. 6b, closed circles) decreased with progressive increases in Mch concentration. Similar decrements were found in $FEV_{0.10}$ (Fig. 6c, closed circles) and $FEV_{0.05}$ (Fig. 6c, open circles). In contrast, $FEV_{0.10}/FVC$ (Fig. 6d, closed circles) and $FEV_{0.05}/FVC$ (Fig. 6d, open circles) increased with increase in Mch concentration.

In Fig. 6b, the position of the peak point (open diamonds) and the inflection point between the second and third phases (open circles) on forced expiratory volume are also drawn. In this analysis the third and fourth phases were not delineated because the fourth phase was not always seen. Although both the position of the peak expiratory flow (open diamonds) and that of the inflection point between the second and third phases (open circles) tended to decrease with increases in inhaled Mch concentration, these changes were negligible compared with decreases in FVC. Thus, decreases in FVC following inhaled Mch were mainly the result of shortening of the third + fourth phases.

In two rats, forced expirations were performed before and after ip pancuronium administration. There was no apparent change in the shape of the *F-V* curve, PEFR, or FVC.

Fig. 6 With an increase in the concentration of inhaled Mch (methacholine), PEFR (**a**), FVC (*filled circles* in **b**), $FEV_{0.10}$ (*filled circles* in **c**), and $FEV_{0.05}$ (*open circles* in **c**) gradually decreased while $FEV_{0.1}$/FVC (*filled circles* in **d**) and $FEV_{0.05}$/FVC (*open circles* in **d**) progressively increased. The inflection point between the second and third phases (*open circles* in **b**) and the position of the peak point (*open diamonds* in **b**) on forced expiratory volume are also shown. Values are mean ± SD. $\$P < 0.05$ versus 0, $*P < 0.05$ versus 0.5, $\#P < 0.05$ versus 1.0, $+P < 0.05$ versus 2.0
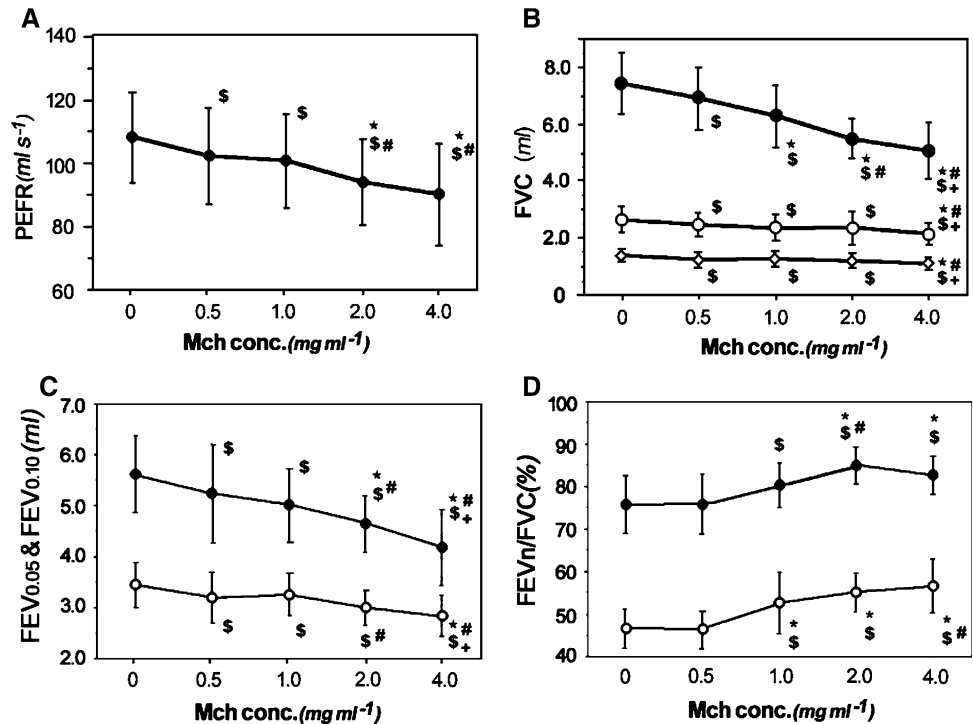
Discussion

Methods

In all previous animal studies [2, 4–6], *F-V* curves were obtained by application of negative pressure to the airway. However we considered this method unsatisfactory for at least two reasons. First, the abrupt opening of the airway shutter in these methods could have provided an explosive initial flow resembling that of a cough [7, 8]. PEFR accompanying a cough is always higher than that of a forced expiration [8]. Second, negative pressure applied to the trachea in these methods was transmitted sequentially to smaller airways and alveoli, and in such a sequence, opposite that of a normal forced expiration, gases in the peripheral airways move later in the expiratory flow. Chest wall compression is a method sometimes applied to infants who do not forcefully exhale [9, 10]. In contrast to the application of negative pressure, our method may have produced a slightly more gradual increase in driving pressure because there is a large dead space, i.e., airtight box and reservoir tank. This may have delayed the occurrence of peak flow. Presumably these physiological differences contributed to a longer ascending phase and higher flow in the descending phases in the *F-V* curves in our study compared with those in previous studies. The differences in lung volume during forced expiration between these two methods should be noted. In our method, gas in the airway and alveoli upstream of the flow limitation point must be compressed during forced expiration and thus exhaled gas volume may be smaller than the exact change in lung volume.

In most of the previous studies on *F-V* curves in small animals, tracheal cannulae with relatively large diameters were used with a tracheostomy. For example, Diamond et al. [2] used a metal cannula with a 2.3 mm diameter in rats (body weight 169–284 g), Hoymann et al. [6] used a cannula with a 1.78 mm ID in rats (body weight ∼248 g), and Lucey et al. [4] used a metal cannula with a 1.5 mm ID in hamsters (body weight 111–145 g). However use of such cannulae with a tracheotomy is less reflective of normal physiologic conditions, and such a procedure is not suitable for repeated measurement of *F-V* curves over an extended period of time. In the present study, we initially determined the maximum size of plastic catheter for oral intubation. Although oral intubation with a 14G catheter (OD 2.0 mm) could easily be accomplished, the catheter exhibited extremely high resistance and the *F-V* curve showed marked delay in the PEFR. A 13G catheter (OD 2.3 mm) was the maximum size for oral intubation. The *F-V* curve using a 13G catheter (OD 2.3 mm) was associated with values of FVC, PEFR, $FEV_{0.05}$, and $FEV_{0.10}$ almost similar to those using a 12G catheter. Delay of the PEFR was significant but the difference was only 0.2 ml. These results suggest that the *F-V* curve using a 13G catheter with oral intubation provides almost the same data as using a 12G catheter with tracheostomy.

We wondered whether abrupt application of positive pressure provoked a compensatory response by the inspiratory muscles although muscle paralysis was not performed in any of the previous studies. Milic-Emili et al. [11] reported that such load compensation was weak in anesthetized animals. We confirmed their opinion by measuring F-V curves before and after muscle paralysis. Inputs from airway mechano-receptors also facilitate respiratory rhythm as the deflation reflex [12]. We excluded this possibility by cervical vagotomy.

Flow-volume curve

In contrast to the F-V curve in humans, the F-V curve in rats consists of four phases. The quadriphasic F-V pattern is not surprising since a similar quadriphasic pattern can be seen in other animals smaller than humans such as dogs [13] and hamsters [4]. In this study we analyzed the third and fourth phases as a single component because the fourth phase was not always observed.

In human studies, the initial half of the F-V curve, i.e., the first and second phases in our study, has been regarded as effort-dependent. The subsequent half of the curve occupying 50–82% of the FVC is effort-independent. However, recent human studies have also suggested that the effort-dependent part of the F-V curve including the PEFR is also limited by a choke point [14–16]. In our study, the PEFR was not affected by changes in driving pressure above 56 cmH$_2$O, and expiratory flow reached PEFR while driving pressure was still increasing. These results suggest that the peak flow in rats was limited by a choke point. Since even in larger animals such as dogs flow limitation can occur at the trachea [7, 13], limitation of the peak flow may occur at the trachea in rats.

Whether flow limitation had been established in the descending limb of F-V curve is also an important matter. Although we did not record F-V curves at lower lung volumes, Diamond and O'Donnel [2] and Leucy et al. [4] have mentioned them. Diamond and O'Donnel [2] compared rat F-V curves breathing either air or He-O$_2$ mixture and found that the increase ($\sim$17%) of flow breathing He-O$_2$ at mid-vital capacity was less than that in humans ($\sim$50%). They speculated that the flow limitation point in this lung volume existed in the relatively small airways. Leucy et al. [4] plotted expiratory flows against driving pressures during forced expiration at several lung volumes in the hamster. They found that maximum expiratory flow was reached at lung volumes as high as 70% vital capacity at a critical driving pressure of -30 cmH$_2$O. When lung volume was lessened, a flow maximum was obtained with less driving pressure. For example at 10% vital capacity, the flow reached its maximum at -5 cmH$_2$O. These

findings suggested that expiratory flow in the descending part of F-V curve was limited by lung volume.

The descending phase of the F-V curve has a complex shape, and this may be explained by the flow limitation mechanism. The initial part of the descending limb represents the flow limitation of larger airways and the latter part represents that in smaller airways [17]. The flow limitation point is not fixed in the airway and moves peripherally during forced exhalation as the lung volume decreases [17]. It is also suggested that the flow limitation point does not move contiguously but jumps from one point to another [18]. We speculated, therefore, that there may be two or three flow limitation points in the F-V curve in rats. As shown in Fig. 6b, only the third + fourth phase was shortened by Mch inhalation. This finding suggests that the bronchoconstrictive effect of inhaled Mch was more pronounced in the mid-sized and smaller airways.

Whether and how inhaled Mch constricted airways should be discussed here. Petak et al. [19] applied Mch inhalation to anesthetized, tracheostomized, and paralyzed rats. They measured airway resistance using a forced oscillation method 30 s after Mch inhalation (0, 1, 2, 4, 8, or 16 mg kg^{-1}). A dose versus response relationship was found between airway resistance and Mch concentration, and airway resistance at highest Mch concentration was almost twice that at baseline. We also measured rat's airway resistance and functional residual capacity by means of body plethysmography [20]. Using Mch concentrations of 0, 0.5, 1.0, 2.0, and 4.0 mg ml^{-1} each for 2 min, the measured parameters increased in a dose-dependent fashion with mean functional residual capacities of 3.77, 4.43, 4.75, 5.02, and 5.34 ml and mean airway resistances of 0.19, 0.22, 0.36, 0.50, and 0.67 cmH$_2$O ml^{-1} s^{-1}, respectively. Measurement after Mch inhalation demonstrated profound bronchoconstriction associated with dose-dependent increases in functional residual capacity.

Cholinergic receptor distribution may be one possible explanation of such selective constriction. However, in vitro studies on muscarinic innervation in small animals are unhelpful. For example, acetylcholine constricted smaller but not large airways in porcine studies [21], while Mch constricted distal bronchioles preferentially in rats [22]. Cholinergic receptors were rich in bronchial airways but sparse in proximal bronchioles in ferrets and guinea pigs [23]. Therefore, airway narrowing is not determined exclusively by muscarinic receptor distribution. Smaller airways are fragile (airway cartilage is sparse), and their resistance to airflow is markedly affected by change in caliber (fourth power of radius change) which is closely related to lung volume. Such anatomical and mechanical factors should also be considered.

Parameters for airway obstruction

PEFR, FVC, $FEV_{0.05}$, and $FEV_{0.10}$ were independent of driving pressure above 56 cmH_2O in the rats. Therefore all of them might be useful parameters for estimation of airway obstruction.

When airways were constricted by inhaled Mch, both PEFR and FVC decreased almost proportionally with the increase in Mch concentration. Thus, as in human studies, PEFR and FVC can reflect airway obstruction. We found that $FEV_{0.05}$ and $FEV_{0.10}$ also decreased proportionally with increase in the concentration of inhaled Mch and can also be useful in this regard. In clinical practice, $FEV_{1.0}$/FVC rather than $FEV_{1.0}$ is used to define obstructive pulmonary impairment. In the present study, $FEV_{0.05}$/FVC and $FEV_{0.10}$/FVC increased with increase in the concentration of inhaled Mch and such a paradoxical increase occurred simply because of a relatively larger decrease in FVC. Therefore we propose that $FEV_{0.05}$ and $FEV_{0.10}$ may be of limited usefulness for this purpose.

As has been discussed, changes in PEFR represent flow limitation in larger airways. On the other hand, the decrease in FVC due to Mch inhalation was largely due to shortening of the third + fourth phase of the *F-V* curve representing flow limitation in smaller airways. We previously measured functional residual capacity (FRC) in rats using a body plethysmograph [20]. FRC in the rats increased by 41% with increase in concentration of inhaled Mch to 4.0 mg ml^{-1}. Stengel et al. [24] also reported similar results. The increase in FRC by a bronchoconstrictive agent is thought to be due to air trapping implying constriction of small airways by Mch inhalation. This may explain the shortening of the third + fourth phase of the *F-V* curve in the present study. Therefore, FVC may also be an optimal parameter for estimating obstructive changes resulting from constriction in mid-sized and small airways.

In conclusion, we utilized a method to obtain the most accurate *F-V* curves and spirograms in unparalyzed and tracheally intubated rats by application of positive pressure to their body surface. PEFR and FVC were the most optimal parameters for the estimation of airway obstruction. PEFR may represent obstruction of larger airways and FVC obstruction of mid-sized and small airways.

References

1. Bates JHT, Irvin CG (2003) Measuring lung function in mice: the phenotyping uncertainty principle. J Appl Physiol 94:1297–1306

2. Diamond L, O'Donnel M (1977) Pulmonary mechanics in normal rats. J Appl Physiol 43:942–948

3. Hohlfeld J, Hoymann HG, Molthan J, Fabel H, Heinrich U (1997) Aerosolized surfactant inhibits acetylcholine-induced airway obstruction in rats. Eur Respir J 10:2198–2203

4. Lucey EC, Celli BR, Snider GL (1978) Maximum expiratory flow and transpulmonary pressure in the hamster. J Appl Physiol 45:840–845

5. Lai Y-L, Chou H-C (2000) Respiratory mechanics and maximal expiratory flow in the anesthetized mouse. J Appl Physiol 88:939–943

6. Hoymann HG, Heinrich U, Beume R, Kilian U (1994) Comparative investigation of the effects of zardaverine and theophylline on pulmonary function in Rats. Exp Lung Res 20:235–250

7. Hayama N, Kondo T, Kobayashi I, Tazaki G, Eguchi K (2003) Effects of bronchial intermittent constrictions on explosive flow during coughing in the dog. Jpn J Physiol 53:71–76

8. Leith DE, Butler JP, Sneddon SL, Brain JD (1986) Cough. In: Fishman AP (ed) Handbook of physiology. Section 3: the respiratory system. Vol. III, part 2: mechanics of breathing. American Physiological Society, Washington DC

9. Tausssig LM, Landau LI, Godfrey S, Arad I (1982) Determinants of forced expiratory flows in newborn infants. J Appl Physiol 53:1220–1227

10. Tepper RS (1987) Airway reactivity in infants: a positive response to methacholine and metaproternol. J Appl Physiol 62:1155–1159

11. Milic-Emili J, Zin WA (1986) Breathing responses to imposed mechanical load. In: Cherniack NS, Widdicombe JG (eds) Handbook of physiology. Section 2: the respiratory system. Vol. II, part 2: control of breathing. American Physiological Society Washington, DC

12. Widdicombe JG (2006) Reflexes from the lungs and airways: historical perspective. J Appl Physiol 101:628–634

13. Pedersen OF, Thiessen B, Lyager S (1982) Airway compliance and flow limitation during forced expiration in dogs. J Appl Physiol 52:357–369

14. Pedersen OF, Brackel HJL, Bogaard JM, Kerrebijn KF (1997) Wave speed-determined flow limitation at peak flow in normal and asthmatic subjects. J Appl Physiol 83:1721–1732

15. Tantucci C, Duguet A, Giampiccolo P, Similowski T, Zelter M, Derenne J-P (2002) The best peak expiratory flow is flow-limited and effort-independent in normal subjects. Am J Respir Crit Care Med 165:1304–1308

16. Aljuri N, Venegas JG, Freitag L (2006) Viscoelasticity of the trachea and its effects on flow limitation. J Appl Physiol 100:384–389

17. Rodarte JR, Rehder K (1986) Dynamics of respiration. In: Fishman AP (ed) Handbook of physiology. Section 3: the respiratory system. Vol. III, part 1: mechanics of breathing. American Physiological Society, Washington DC

18. Mead J (1980) Expiratory flow limitation: a physiologist's point of view. Fed Proc 39:2771–2775

19. Petak F, Hantos Z, Adamicza A, Asztalos T, Sly P (1997) Methacholine-induced bronchoconstriction in rats: effects of intravenous vs. aerosol delivery. J Appl Physiol 82:1479–1487

20. Kondo T, Tanigaki T, Tsuji C, Ishii H, Tazaki G, Kondo Y (2009) Aerosolized methacholine induced bronchoconstriction and pulmonary hyperinflation in rats. J Phyiol Sci 59:347–353

21. Mitchell HW, Cvetkovski R, Sparrow MP, McFawn PK (1998) Concurrent measurement of smooth muscle shortening, lumen narrowing and flow to acetylcholine in large and small bronchi. Eur Respir J 12:1053–1061

22. Kott KS, Pinkerton KE, Bric JM, Plopper CG, Avandhanam KP, Joad JP (2002) Methacholine responsiveness of proximal and

distal airways of monkeys and rats using videomicrometry. J Appl Physiol 92:966–989

23. Barnes PJ (2004) Distribution of receptor targets in the lung. Proc Am Thorac Soc 1:345–351

24. Stengel PW, Yiamouyiannis CA, Obenchain RL, Cockerham SL, Silbaugh SA (1994) Methacholine-induced pulmonary gas trapping in guinea and rats. Exp Lung Res 20:235–250